Nickel-Templated Replacement of Phosphine Substituents in a Tetradentate Bis(amido)bis(phosphine) Ligand

Kyounghoon Lee† and Christine M. Thomas*

Department of Chemistry and Biochemistry, The Ohio State University, Columbus, OH 43210, United States

Supporting Information Placeholder

ABSTRACT: The replacement of phosphine substituents in nickel-bound PNNP ligands is reported as an alternative method to prepare multidentate phosphine ligands with alkyl substituents. Treatment of the previously reported bis(phosphide) complex $\{K(THF)_x\}_2{}^{2Ph}$[PNNP]Ni (**2**) with two equivalents of MeI, ^{i}PrI, or 1,3-dibromoethane formed alkyl-substituted complexes ^{2Ph,2Me}[PNNP]Ni (**3**), ^{2Ph,2iPr}[PNNP]Ni (**4**), and ^{2Ph,propylene}[PNNP]Ni (**5**), respectively. The stereoselectivity (racemic vs. meso) of these reactions can be controlled by varying the reaction temperature. The racemic mixture of products with the new alkyl substituents in an *anti* configuration were favored at lower temperature, whereas a larger proportion of meso compounds was acquired at higher temperature. Further treatment of **3** with KH resulted in selective elimination of the remaining phenyl groups rather than the methyl substituents, affording bis(methylphosphide) complex $\{K(THF)_x\}_2{}^{2Me}$[PNNP]Ni (**6**). Subsequent treatment of **6** with additional MeI formed ^{4Me}[PNNP]Ni (**7**), in which all four phenyl groups were replaced with methyl substituents. As a proof of concept, demetallation of the ligand from **7** was achieved using aqueous KCN to form a free dimethylphosphine-substituted ligand $H_2{}^{4Me}$[PNNP] (**8**), and **8** was subsequently coordinated to a different metal, using $PdCl_2$ to form ^{4Me}[PNNP]Pd (**9**). Unlike the clean elimination of phenyl substituents from **3**, the reactions of KH with **4** and **5** exhibited competitive elimination of both alkyl and phenyl substituents and/or attenuated reactivity.

Introduction

Phosphine ligands have been extensively used in homogeneous catalysis and organometallic chemistry due to their strong donor ability and tunability.[1–3] The electronic and steric properties of phosphines can be tuned by altering the substituents and compared using Tolman's electronic parameter (TEP) and cone angle.[4,5] The incorporation of phosphine donor fragments into multidentate chelating ligands results in more stable transition metal complexes and further enhances their utility. Multidentate phosphine ligands are typically prepared via one of the following routes: (1) nucleophilic substitution of halogenophosphine fragments with RLi or Grignard reagents, (2) nucleophilic substitution of RX (X = halide) functionalities with alkali metal phosphide reagents, (3) hydrophosphination of unsaturated compounds, (4) reduction of P(V) compounds, and (5) functionalization of existing phosphine substituents.[1–3,6] The one commonality between these synthetic routes is that they require reagents containing chemically reactive P-X or P-H bonds that are typically challenging to work with and often difficult to obtain commercially or synthesize on a large scale. For example, PMe_2-substituted phosphine ligands may be attractive ligand platforms for some applications due to their minimal steric bulk and strong σ-donating ability, but their preparation renders them unappealing targets because of the volatility, toxicity, air-sensitivity, and cost of the requisite ligand precursor $ClPMe_2$.[6,7] Moreover, the aforementioned synthetic routes are often problematic when preparing multidentate phosphine ligands containing other reactive functional groups (e.g. primary or secondary amines).[8] Yet another complication arises when synthesizing multidentate phosphine-containing ligands with different substituents PR^1R^2, as the P-stereogenic phosphorus centers result in a mixture of stereoisomers that are challenging to separate.[3,9]

Tetradentate PNNP ligands and their transition metal complexes have been prepared and used in catalysis[10–14] and photoluminescence,[15] and as building blocks for bimetallic complexes.[16,17] Our research group recently reported the coordination of a bis(amido)bis(phosphine) ^{4Ph}[PNNP]$^{2-}$ ligand to Ni and Fe and the metal-ligand cooperativity of the ^{4Ph}[PNNP]Fe complex.[18,19] We have shown that phenyl substituents in the ^{4Ph}[PNNP]$^{2-}$ ligand can be readily eliminated using potassium hydride when the ligand is bound to nickel ^{4Ph}[PNNP]Ni (**1**), affording the bis(amido)bis(phosphido) complex $\{K(THF)_x\}_2{}^{2Ph}$[PNNP]Ni (**2**) shown in Scheme 1.[18] P-C bond cleavage is well-known to occur when tertiary phosphines are treated with alkali metals to form alkali metal phosphides.[20–22] Han and coworkers recently reported the use of this reaction in the preparation of organophosphines via addition of ArCl reagents to *in situ*-generated alkali metal phosphides.[22] Inspired by this report, we hypothesized that the treatment of **2** with RX electrophiles could be used to selectively install new phosphine substituents on the tetradentate [PNNP]$^{2-}$ framework, allowing us to synthesize more electron-rich alkyl-substituted ligand derivatives that we have been unable to synthetically access via other methods.

Herein, we describe the nickel-templated replacement of the phenyl phosphine substituents in ^{4Ph}[PNNP]$^{2-}$ to form new tetradentate ligands/complexes with P-methyl or P-isopropyl substituents as well as a propylene-bridged macrocyclic complex. We demonstrate that control of the reaction temperature can tune the relative ratio of stereoisomers as supported by both experimental and computational studies. In addition, all four of the phenyl substituents in **1** can be replaced with methyl groups to form PMe_2-substituted complexes and ligands, which showcases the safer and more economical preparation of substituted multidentate phosphines whose syntheses would be otherwise challenging.

Results and Discussion

First, the addition of methyl substituents to **2** was investigated using MeI (Scheme 1). Treatment of **2** with 2.5 equivalents of MeI in THF at room temperature afforded a red-orange solution with white precipitate. Two singlet resonances were observed at 25.2 and 25.5 ppm in the $^{31}P\{^{1}H\}$ NMR spectrum with relative integrations of 0.66:0.34 (Figure S5). Two multiplets associated with the Me groups attached to the phosphorus atoms were observed at 1.26 and 1.90 ppm in the ^{1}H NMR spectrum with the same ratio (Figure S4). As the temperature at which MeI was added was decreased, the fraction of the species with a $^{31}P\{^{1}H\}$ NMR chemical shift at 25.2 ppm increased, ultimately reaching 0.98:0.02 when MeI was added to a frozen solution of **2** in THF at around -100 °C (Figure S26). The major product was a racemic mixture (**3**^{rac}) of ^{2Ph,2Me}[PNNP]Ni (**3**), with the newly installed Me substituents oriented in an *anti* configuration with respect to the square plane, as confirmed by single crystal X-ray diffraction (Figure 1). The Ni(II) center of **3**^{rac} adopts a square planar geometry with comparable Ni-N bond distances and 0.03 – 0.04 Å shorter Ni-P bond distances in comparison to **1** (Table 1).[18] Given that diphosphines with two stereogenic phosphorus centers generally form racemic mixture and meso isomers,[3,9] we tentatively assigned the other species as a meso compound **3**^{meso} (Figure 1) in which the two new Me substituents are oriented in the same direction with respect to the square plane. Complex **3**^{rac} can be prepared in comparable yield (74% vs 81%) in a one-pot synthesis by the treatment of **1** with 3 equivalents of KH in THF at 50 °C, filtration of the reaction mixture, and subsequent treatment with 2.5 equivalents of MeI (Scheme 1).

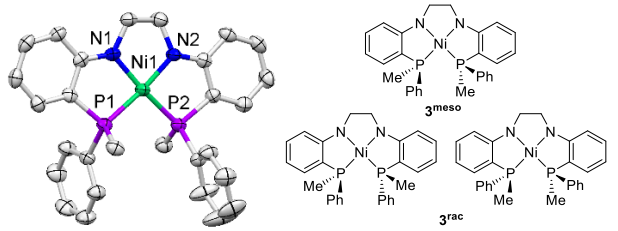

Figure 1. Solid-state structure of **3**^{rac} (*left*) with ellipsoids drawn at the 50% probability level and stereoisomers of **3** (*right*). For clarity, only one of two independent molecules in the asymmetric unit of **3**^{rac} is shown and hydrogen atoms were omitted.

Subsequently, density functional theory (DFT) calculations were carried out to investigate the factors that lead to the formation of **3**^{rac} and **3**^{meso} (Table S3). The geometry optimization exhibited that the free energy of **3**^{rac} is 1.4 kcal/mol lower than that of **3**^{meso}. However, we anticipate that direct epimerization of **3**^{rac} and **3**^{meso} is highly unfavorable, as this process would require both phosphine dissociation and stereoinversion at phosphorus, so the ratio of **3**^{rac} and **3**^{meso} is likely determined by intermediates prior to P-C bond formation. The phosphorus centers of the dianionic bisphosphide complex **2** adopt a pyramidal geometry without any π-bonding interactions to nickel.[18] As a result of the stereochemically active lone pairs on phosphorus, **2** can adopt either *syn* or *anti* geometries, with two enantiomers possible for the *anti* geometry. Optimization of the *syn* and *anti* geometries of **2** revealed the *anti* geometry to be 3.2 kcal/mol lower in free energy. The first equivalent of Me^+ generates ^{2Ph,Me}[PNNP]Ni$^-$, which can also exist with the Ph groups oriented in a *syn* or *anti* fashion. It was, again, found that the *anti* orientation was slightly lower in free energy (1.3 kcal/mol) relative to the *syn* counterpart. The second equivalent of Me^+ is therefore more likely to encounter the thermodynamically preferred *anti* intermediate, favoring the formation of **3**^{rac}. However, the free energy differences between these the *syn* and *anti* geometries are relatively small, and the relative orientation of the Ph groups in the mono(phosphide) intermediate ^{2Ph,Me}[PNNP]Ni$^-$ can be readily interconverted through a transition state with a barrier of just 16.4 kcal/mol. These data are, therefore, consistent with the observation that lower reaction temperatures are required to fully favor the formation of **3**^{rac} rather than a mixture of **3**^{rac} and **3**^{meso}.

Scheme 1.

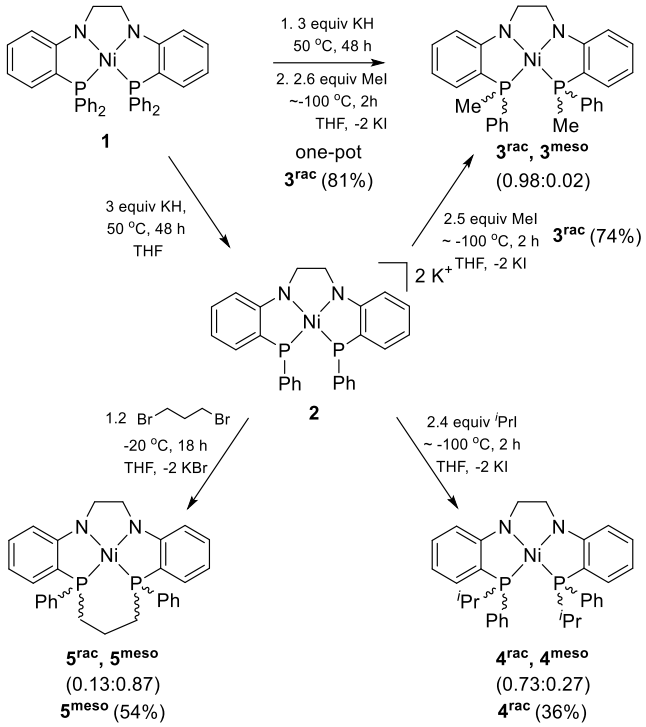

To assess the generality of our procedure for replacing phenyl groups with alkyl substituents, we attempted a reaction of **2** with ^{i}PrI (Scheme 1). Treatment of **2** with 2.5 equivalents of ^{i}PrI at room temperature resulted in the appearance of two singlets in the $^{31}P\{^{1}H\}$ NMR spectrum at 49.2 and 49.3 ppm with relative integrations of 0.67:0.33. The small difference in chemical shift and the relative ratio of the two products was remarkably similar to that of the MeI reaction. In this case, however, decreasing the reaction temperature proved ineffective at favoring a single product: Adding ^{i}PrI to a frozen solution of **2** in THF still resulted in a mixture of products in a 0.73:0.27 ratio (Figure S27). The major product was successfully isolated via crystallization from Et_2O, and single crystal X-ray diffraction confirmed that the favored isomer exists as a racemic mixture isomer (**4**^{rac}) of ^{2Ph,2iPr}[PNNP]Ni (**4**) with the Ph groups oriented in an *anti* configuration (Figure 2).

Both the MeI and ^{i}PrI reactions with **2** favor the racemic mixture of products with Ph groups oriented on opposite sides of the square plane (**3**^{rac} and **4**^{rac}); however, the inability to influence the ratio of **4**^{rac}/**4**^{meso} was a clear difference we sought to understand. DFT calculations were carried out (Table S4), but the results were largely similar to those described for **3**^{rac}/**3**^{meso} and did not shed light on the experimental observations. Ultimately, we attribute the observed difference in the ratio of rac/meso products between MeI (0.98:0.02) and ^{i}PrI

Table 1. Selected bond distances (Å) and angles (°) from single crystal X-ray diffraction data.

	1[18]	**3**^{rac}		**4**^{rac}	**5**^{meso}	**6**	
Ni-P	2.1675(5)	2.1328(9)	2.1291(9)	2.1448(5)	2.112(1)	2.179(2)	2.162(2)
		2.1385(9)	2.1353(9)		2.112(1)	2.181(2)	2.178(2)
Ni-N	1.867(2)	1.858(2)	1.853(2)	1.865(2)	1.850(3)	1.882(6)	1.870(6)
		1.858(2)	1.856(2)		1.865(4)	1.883(6)	1.887(6)
P-Ni-P	102.97(3)	101.45(3)	102.10(3)	101.00(3)	95.89(5)	100.88(8)	100.02(8)
N-Ni-N	85.07(9)	86.0(1)	86.2(1)	86.2(1)	86.9(2)	85.6(3)	85.0(3)

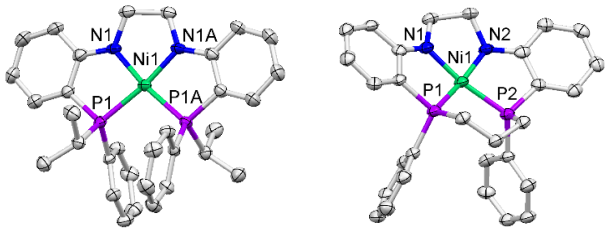

Figure 2. Solid-state structures of **4**^{rac} (*left*) and **5**^{meso} (*right*) with ellipsoids drawn at the 50% probability level . Co-crystallized solvent molecules and hydrogen atoms were omitted for clarity.

(0.73:0.27) in reactions carried out at low temperature to the intrinsic electrophilicity of Me^+ vs. $^iPr^+$. Since MeI is a stronger electrophile, its reaction with anionic phosphide fragments is likely more rapid at low temperature when intermediates with *anti* geometry are more favored to preferentially form **3**^{rac}. The less electrophilic ^{i}PrI, on the other hand, may not begin reacting appreciably with ^{2Ph,iPr}[PNNP]Ni$^-$ until the reaction mixture has warmed to a temperature where the fraction of the *syn* intermediate of ^{2Ph,iPr}[PNNP]Ni$^-$ is higher. Consistent with electrophilicity arguments, aryl iodides, which are even less electrophilic, do not react appreciably with **2.**

We then turned our attention to the reactivity of **2** with a dihaloalkane to determine whether macrocyclic complexes can be prepared using the same approach (Scheme 1). The addition of 1.2 equivalents of 1,3-dibromopropane to **2** at -20 °C generated a mixture of products with two sharp singlets at 34.7 and 29.4 ppm in a 0.13:0.87 integral ratio in the $^{31}P\{^1H\}$ NMR spectrum. The major product was isolated via crystallization, and single crystal X-ray diffraction data revealed it to be the isomer (**5**^{meso}) of ^{2Ph,propylene}[PNNP]Ni (**5**), with both Ph groups oriented on the same side of the molecule as shown in Figure 2. The square planar geometry about the Ni(II) center is maintained in **5**^{meso} and the propylene linker between the two phosphine donors results in a P-Ni-P bite angle of 95.89(5)° that is 6° smaller in comparison to **3**.

To explore the origin of the preferential formation of the meso isomer of **5**, the effect of reaction temperature on product distribution was explored (Figure S28). Performing the addition of 1,3-dibromopropane to **2** at -78 °C and allowing the reaction to warm immediately to room temperature afforded a mixture of **5**^{rac} and **5**^{meso} in a 0.12:0.88 ratio. When the reaction was again performed at -78 °C at the same concentration but on twice the scale, the ratio of **5**^{rac} to **5**^{meso} increased to 0.35:0.65. We posited that the increased fraction of **5**^{rac} resulted from slower warming due to the increased solvent volume. To test this hypothesis, 1,3-dibromopropane was again added to **2** at -78 °C, this time keeping the reaction in the cold bath and allowing it to warm to room temperature more slowly. The ratio of **5**^{rac} to **5**^{meso} increased even further to 0.43:0.57 under these reaction conditions. The observed variations in product ratio and the preference for the *anti*/meso product originates from the relative energy differences between the intermediate singly alkylated isomers and the final products **5**^{rac} and **5**^{meso} (Table S5). Unlike the aforementioned alkyl halide reactions, **5**^{meso} was found to be 13.0 kcal/mol more stable than **5**^{rac}. By analogy to ^{2Ph,Me}[PNNP]Ni$^-$, we anticipate the *anti* conformation of the singly alkylated intermediate to be more stable. However, unlike the aforementioned alkyl halide reactions, the subsequent alkylation is an intramolecular process. At higher temperatures, the *syn*/*anti* isomerization process is thermodynamically accessible for the singly alkylated intermediate, allowing the more stable **5**^{meso} isomer to form. However, when a lower reaction temperature is maintained, the intramolecular electrophilic attack of the second alkyl bromide fragment occurs on a faster timescale than *syn*/*anti* isomerization, allowing **5**^{rac} to form from more stable *anti* intermediates.

Seeking to further modify the phosphine substituents, we studied the further reactivity of **3** (the mixture of **3**^{rac} and **3**^{meso}) to determine whether the second phenyl group could be eliminated. Heating **3** with three equivalents of KH in THF at 50 °C for 72 h afforded a product with a broad singlet at -3.5 ppm in its $^{31}P\{^1H\}$ NMR spectrum (Scheme 2). The observed 29 ppm upfield shift was comparable to that observed upon the phenyl elimination from **1** to form **2** (25 ppm upfield shift).[18] In addition, the ^1H NMR spectrum of the isolated product contained only 8 aromatic protons compared to the 18 aromatic protons of **3**, consistent with the loss of two phenyl groups. Phenyl group elimination was confirmed by single crystal X-ray diffraction of the product $\{K(THF)_x\}_2{}^{2Me}$[PNNP]Ni (**6**) (Figure 3). The exclusive formation of **6** unequivocally shows that phenyl groups are preferentially eliminated over methyl substituents.

The reaction of bis(phosphide) complex **6** with alkyl halide electrophiles was next explored to determine whether additional alkyl substituents could be added. Indeed, the addition of 2.5 equivalents of MeI to **6** affords a single product with a sharp singlet at 13.5 ppm in its $^{31}P\{^1H\}$ NMR spectrum. The high-resolution ESI-MS spectrum of the product reveals an *m/z* value (389.0850) and isotopic pattern consistent with the $[M+H]^+$ ion of the tetramethylated bis(amido)bis(phosphine) complex ^{4Me}[PNNP]Ni (**7**). This assignment was further supported by the absence of P-Ph resonances in the ^1H NMR spectrum and the presence of a doublet that integrates to 12 protons and corresponds to PMe_2 substituents. Furthermore, **7** could be prepared in a stepwise one-pot synthesis from **3** via treatment with three equivalents of KH at 50 °C in THF followed by the

filtration of the reaction mixture and treatment of the filtrate with 2.5 equivalents of MeI. Overall, the sequence of reactions from **1** to **3** to **7** provides a successful Ni-templated pathway to replace all of the P-Ph substituents with P-Me substituents to afford a new nickel complex with a tetradentate PMe_2-substituted $[PNNP]^{2-}$ ligand that would be challenging to synthesize by other means.

Scheme 2.

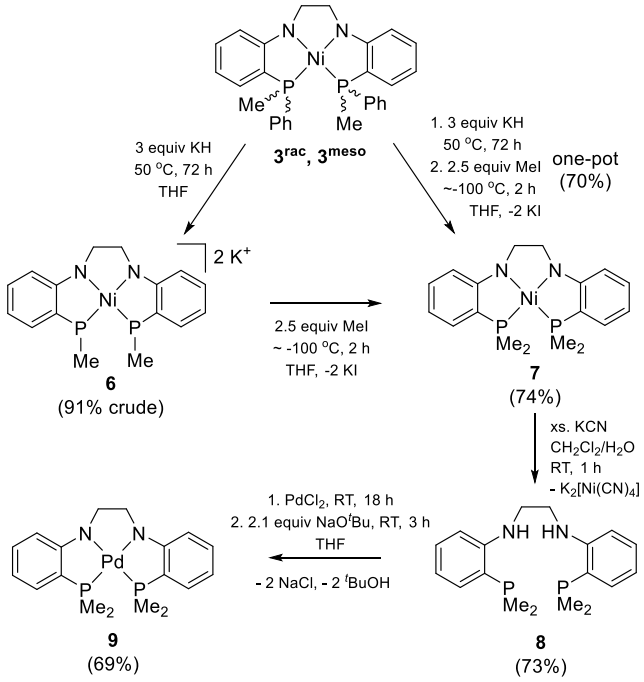

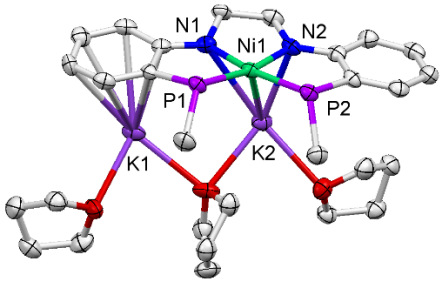

Figure 3. Solid-state structure of 6 with ellipsoids drawn at the 50% probability level. For clarity, only one of two independent molecules in the asymmetric unit is shown and hydrogen atoms were omitted.

The broad utility of a Ni-templated ligand synthesis route hinges on the ability to remove the Ni and replace it with other metals. Therefore, we next investigated whether nickel could be removed from complex **7** (Scheme 2). Previous reports have demonstrated the effective removal of Ni from macrocyclic ligands using excess cyanide salts, eliminating $Ni(CN)_4^{2-}$.[23–26] A solution of **7** in CH_2Cl_2 was treated with a solution of excess KCN in degassed H_2O. The organic layer became colorless while the aqueous layer turned orange-yellow. The $^{31}P\{^1H\}$ NMR spectrum of the organic layer featured a sharp singlet at -68.6 ppm and the ^1H NMR spectrum of the isolated product exhibited a signal consistent with amine protons at 5.31 ppm. The observed spectroscopic variations in conjunction with the loss of color correspond to the demetallation of **7** and formation of $H_2{}^{4Me}$[PNNP] (**8**). This transformation was further verified by elemental microanalysis and high-resolution ESI-MS.

As a further proof of principle, the free ligand **8** was coordinated to a different transition metal (Scheme 2). Treatment of **8** with $PdCl_2$ and 2 equivalents of NaO^tBu in THF generated ^{4Me}[PNNP]Pd (**9**) as a yellow compound with a single $^{31}P\{^1H\}$ NMR resonance at 9.4 ppm. The formation of **9** was fully supported by NMR spectroscopy, elemental microanalysis, and high resolution ESI-MS. Overall, we were able to demonstrate that the phenyl substituents of **1** can be replaced with methyl groups by the repeated treatment of KH and MeI and that nickel can then be replaced with other metals by treatment with excess KCN and subsequent metalation using a different metal precursor.

Scheme 3.

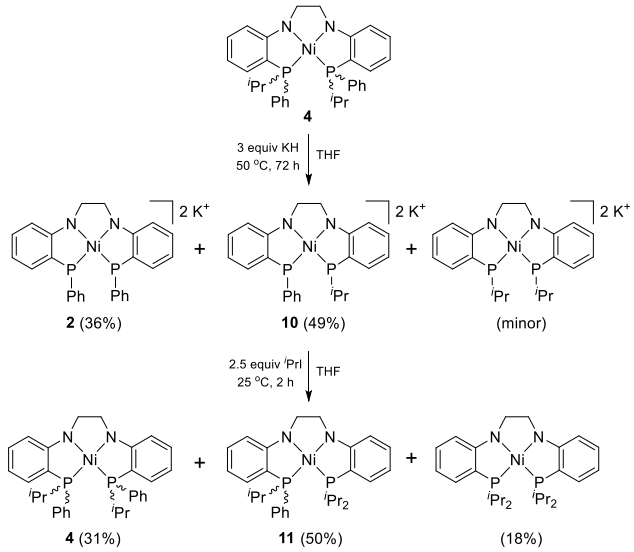

A similar synthetic route to replace both phenyl substituents of **1** with isopropyl groups proved less straightforward. The reaction of **4** with three equivalents of KH in THF at 50 °C resulted in the formation of multiple species based on the $^{31}P\{^1H\}$ NMR spectrum (Figure S29). Unlike the reaction of KH with **3**, the generation of a mixture of products suggests that both phenyl and isopropyl substituents were eliminated to some extent in this case (Scheme 3). Of the three possible products of this reaction, **2**, which results from loss of the two isopropyl groups, was identified by a $^{31}P\{^1H\}$ NMR signal at 14.4 ppm as roughly 36% of the mixture. The major product, however, has two $^{31}P\{^1H\}$ NMR signals at 8.5 and 60.8 ppm that integrate in a 1:1 ratio and is therefore assigned as ^{Ph,iPr}[PNNP]Ni^{2-} (**10**), in which one phenyl and one isopropyl group have been eliminated from **4**. The desired product, ^{2iPr}[PNNP]Ni^{2-}, in which the two remaining phenyl groups have been selectively removed, is not observed in appreciable quantities. Treatment of the aforementioned reaction mixture with 2.5 equivalents of ^{i}PrI further confirmed the assignment of the products of the reaction of **4** with KH (Figure S30). The $^{31}P\{^1H\}$ NMR spectrum contained three singlets at 56.5, 49.5, and 49.2 ppm and two doublets at 58.2 and 48.8 ppm with the coupling constant of 52 Hz each. The two singlet resonances at 49.5 and 49.2 ppm correspond to $\mathbf{4}^{meso}$ and $\mathbf{4}^{rac}$, respectively, which are formed by the addition of ^{i}Pr substituents to **2**. These products account for roughly 31% (10% for $\mathbf{4}^{meso}$ and 21% for $\mathbf{4}^{rac}$) of the reaction mixture, consistent with the ratio of **2** formed in the previous reaction with KH. The two doublets at 58.2 and 48.8 ppm constitute ~50% of the reaction mixture and are tentatively assigned as ^{Ph,3iPr}[PNNP]Ni (**11**), formed via electrophilic addition of the

isopropyl groups to **10,** based on their identical coupling constants (52 Hz) and integrations. The remaining singlet in the $^{31}P\{^{1}H\}$ NMR spectrum at 56.5 ppm may correspond to $^{4i\text{Pr}}$[PNNP]Ni formed from $^{2i\text{Pr}}$[PNNP]Ni^{2-}. This minor product represents < 20% of the reaction mixture. Altogether, it can be concluded that, unlike the selective elimination of phenyl vs methyl substituents in **3**, the elimination of isopropyl groups is competitive with phenyl group elimination in the case of **4**. This observation is comparable to the reported substituent elimination propensity from tri-substituted phosphines, where the relative preference for elimination of ^{i}Pr vs Ph is 0.27:0.73.[22]

Lastly, the reactivity of the macrocyclic complex **5** with excess KH was tested to determine whether the remaining phenyl substituents could be removed/replaced in this case. Upon heating **5** with three equivalents of KH 50 °C in THF for 72 h, no reaction was observed.

Conclusion

In summary, we have shown that the phenyl groups in $^{4\text{Ph}}$[PNNP]Ni (**1**) can be successfully replaced with alkyl substituents by sequential treatment with KH and alkyl halides such as MeI, ^{i}PrI , and 1,3-dibromopropane to form $^{2\text{Ph,2Me}}$[PNNP]Ni (**3**), $^{2\text{Ph,2}i\text{Pr}}$[PNNP]Ni (**4**) and $^{2\text{Ph,propylene}}$[PNNP]Ni (**5**), respectively. The monosubstituted alkyl halides preferentially formed racemic mixtures where the added alkyl groups are oriented anti to each other, whereas 1,3-dibromopropane addition favored the meso product in which the two ends of the propylene linker added to the same face of the molecule. The relative formation of racemic mixture vs. meso isomers can be regulated by varying the temperature at which the reagents are mixed: the racemic mixtures were dominant when reactions were performed at lower temperature while meso compounds were favored with higher reaction temperature. The remaining phenyl groups in **3** were selectively eliminated in a second KH addition step, allowing the preparation of the PMe_2-substituted $^{4\text{Me}}$[PNNP]Ni complex (**7**). Nickel was successfully demetallated using excess cyanide to release the free ligand $H_2{}^{4\text{Me}}$[PNNP] (**8**), and the further coordination of this new ligand to another metal was demonstrated using $PdCl_2$ to form $^{4\text{Me}}$[PNNP]Pd (**9**). Overall, these steps comprise a successful nickel-templated strategy for the construction of a chelating phosphine ligand with different phosphine substituents, which would be challenging and/or expensive to synthesize via other means. Thus far, it appears that limitations to this method may arise from challenges associated with the selective removal of the second set of phenyl groups from derivatives such as **4** or **5**. There are still outstanding fundamental questions about the mechanism by which P-C bond cleavage from **1**, **3**, or **4** occurs, and understanding this process may aid in the development of more selective substituent replacement methods. Future studies will be focused on probing the mechanism by which phosphine substituents are released in the presence of KH and developing alternative protocols to further expand this nickel-templated phosphine substituent modification pathway.

Experimental

General Considerations. All manipulations were carried out under an inert atmosphere using a nitrogen-filled glovebox or standard Schlenk techniques unless otherwise noted. All glassware was oven-dried prior to use. All solvents were degassed by sparging with ultra-high purity argon and dried via passage through columns of drying agents using a Seca solvent purification system from Pure Process Technologies. C_6D_6, CD_3CN, and CD_2Cl_2 were dried over CaH_2, distilled, degassed by repeated freeze-pump-thaw cycles, and stored over pre-activated 3 Å molecular sieves. THF-d_8 was dried over Na/benzophenone, distilled, degassed by freeze-pump-thaw cycles, and stored over pre-activated 3 Å molecular sieves. $^{4\text{Ph}}$[PNNP]Ni (**1**), $\{K(THF)_x\}_2{}^{2\text{Ph}}$[PNNP]Ni (**2**) and neat KH were prepared following our previous report.[18] MeI and ^{i}PrI were dried over P_2O_5, distilled, and stored in the dark at -35 °C under N_2. 1,3-Dibromopropane was distilled and stored under N_2. All other chemicals were purchased from commercial vendors and used without further purifications.

Spectroscopic Characterization and Physical Measurements. ^{1}H and ^{31}P NMR data were recorded on a Bruker DPX-400 instrument operating at 400 MHz for ^{1}H and 162.0 MHz for ^{31}P. ^{13}C NMR data were acquired on a Bruker AVANCE III HD 600 instrument operating at 150.9 MHz. Chemical shifts are reported in δ units in ppm referenced to residual solvent peaks (^{1}H and ^{13}C) or to an 85% H_3PO_4 external standard (^{31}P; δ 0.0). Elemental microanalysis data (CHN) were collected by Midwest Microlab, Indianapolis, IN. High-resolution MS data were obtained using a Bruker Impact II instrument (Bruker Daltronics) with an electrospray ionization (ESI) source and quadrupole time-of-flight (Q-TOF) analyzer system.

$^{2\text{Ph,2Me}}$[PNNP]Ni (3). To a frozen solution of **2** (0.20 g, 0.32 mmol) in THF (20 mL) inside a liquid N_2-cooled cold well was added MeI (0.12 g, 0.85 mmol). The mixture was allowed to warm to room temperature and stirred for 2 h, resulting in the formation of a red-orange solution and a white precipitate. The reaction mixture was filtered through a pad of Celite and the filtrate was evaporated to dryness under vacuum. The residue was extracted with Et_2O (10 mL) and filtered through a pad of Celite. The filtrate was evaporated to dryness under vacuum and dissolved in benzene (*ca.* 2 mL). The diffusion of pentane vapor into the benzene solution yielded red-orange needles and blocks. Yield: 0.12 g (74%). **Alternative one-pot synthesis**: A mixture of **1** (0.20 g, 0.31 mmol) and KH (0.038 g, 0.95 mmol) in THF (20 mL) was heated at 50 °C for 48 h. The reaction mixture was filtered through a pad of Celite and the filtrate was frozen inside a liquid N_2-cooled cold well. MeI (0.11 g, 0.77 mmol) was added, and the mixture was allowed to warm to room temperature. The reaction mixture was stirred for 2 h and filtered through a pad of Celite. The filtrate was evaporated to dryness under vacuum. The residue was extracted with Et_2O (10 mL) and filtered through a pad of Celite. The filtrate was evaporated to dryness under vacuum and dissolved in benzene (*ca.* 2 mL). The diffusion of pentane vapor into the benzene solution yielded red-orange needles and blocks. Yield: 0.13 g (81%). X-ray quality single crystals for the major product (**3$^{\text{rac}}$**) were obtained by the diffusion of pentane vapor into a concentrated solution of **3** in Et_2O. Anal. Calcd for $C_{28}H_{28}N_2NiP_2$: C, 65.53; H, 5.50; N, 5.46. Found: C, 65.60; H, 5.79; N, 5.29. ^{1}H NMR for **3$^{\text{rac}}$** (CD_3CN, 400 MHz): δ 7.61 (m, P-Ph, 4H), 7.52 – 7.43 (m, P-Ph, 6H), 7.03 (m, Ar-H, 2H), 6.72 (m, Ar-H, 2H), 6.33 (m, Ar-H, 2H), 6.15 (m, Ar-H, 2H), 3.49 (m, NCH_2, 4H), 1.25 (m, PMe_2, 6H). $^{13}C\{^{1}H\}$ NMR for **3$^{\text{rac}}$** (CD_3CN, 150.9 MHz): δ 166.0 (vt, $^{2}J_{PC}$ = 13 Hz), 134.1 (s), 133.8 (vt, $^{1}J_{PC}$ = 23 Hz), 132.1 (s), 131.8 (vt, $^{2}J_{PC}$ = 5 Hz), 131.5 (s), 129.9 (vt, $^{2}J_{PC}$ = 5 Hz), 121.2 (vt, $^{1}J_{PC}$ = 29 Hz), 113.0 (s), 109.7 (vt, J_{PC} = 8 Hz), 54.7 (s, N*C*H_2), 9.4 (vt, $^{1}J_{PC}$ = 15 Hz, PMe). $^{31}P\{^{1}H\}$ NMR for **3$^{\text{rac}}$** (CD_3CN, 162.0 MHz): δ 26.0 (s). ESI-MS *m/z*: calcd for $C_{28}H_{29}N_2NiP_2$ 513.1159; found 513.1160.

$^{2\text{Ph,2}i\text{Pr}}$[PNNP]Ni (4). To a frozen solution of **2** (0.10 g, 0.16 mmol) in THF (10 mL) inside a liquid N_2-cooled cold well was added ^{i}PrI (0.067 g, 0.39 mmol). The reaction was allowed to warm to room temperature and stirred for 2 h. The resulting dark brown-orange solution with white precipitate was filtered

through a pad of Celite and the filtrate was evaporated to dryness under vacuum. The product was extracted with Et_2O (5 mL) and filtered through a pad of Celite. The filtrate was reduced in volume to *ca.* 1 mL under vacuum. The Et_2O solution was layered with pentane and stored at -35 °C to yield dark brown solids. Yield: 0.052 g (58%; $\mathbf{4}^{rac}$:$\mathbf{4}^{meso}$ = 0.76:0.24). The major product ($\mathbf{4}^{rac}$) could be isolated by storing the solution in Et_2O (*ca.* 4 mL) at -35 °C to form dark orange brown needles. Yield: 0.033 g (36%). X-ray quality single crystals were obtained by storing the concentrated solution of $\mathbf{4}^{rac}$ in Et_2O at -35 °C. Anal. Calcd for $C_{32}H_{36}N_2NiP_2$: C, 67.51; H, 6.37; N, 4.92. Found: C, 67.03; H, 6.38; N, 4.98. ^{1}H NMR for $\mathbf{4}^{rac}$ (C_6D_6, 400 MHz): δ 7.28 (m, P-Ph, 6H), 7.00 (m, overlapping P-Ph and Ar-H, 6H), 6.68 (m, Ar-H, 2H), 6.64 (m, Ar-H, 2H), 6.36 (m, Ar-H, 2H), 3.77 (m, NCH_2, 2H), 3.60 (m, NCH_2, 2H), 1.44 (m, CH_3CHCH_3, 2H), 1.14 (m, CH_3, 6H), 0.86 (m, CH_3, 6H). ^{13}C{^{1}H} NMR for $\mathbf{4}^{rac}$ (C_6D_6, 150.9 MHz): δ 167.9 (vt, $^1J_{PC}$ = 13 Hz), 134.4 (s), 134.0 (s), 132.4 (m), 132.1 (vt, $^2J_{PC}$ = 4 Hz), 129.9 (s), 128.6 (vt, $^2J_{PC}$ = 4 Hz), 114.2 (m), 111.8 (s), 109.8 (vt, $^2J_{PC}$ = 8 Hz), 54.5 (s, N*C*H$_2$), 24.3 (vt, $^1J_{PC}$ = 13 Hz, P*C*H(CH$_3$)$_2$), 19.3 (s, PCH(*C*H$_3$)$_2$), 17.1 (s, PCH(*C*H$_3$)$_2$). ^{31}P{^{1}H} NMR for $\mathbf{4}^{rac}$ (C_6D_6, 162.0 MHz): δ 49.3 (s). ESI-MS *m/z*: calcd for $C_{32}H_{36}N_2NiP_2$ 568.1707; found 568.1708.

^{2Ph,propylene}[PNNP]Ni (5). To a stirring solution of **2** (0.10 g, 0.16 mmol) in THF (5 mL) was added a solution of 1,3-dibromopropane (0.038 g, 0.19 mmol) in THF (5 mL) at -20 °C. The mixture was allowed to warm to room temperature and stirred overnight. The resulting orange solution with white precipitate was evaporated to dryness under vacuum. The residue was extracted with CH_2Cl_2 (10 mL) and filtered through a pad of Celite. The filtrate was reduced in volume to *ca.* 2 mL under vacuum, layered with Et_2O, and stored at -20 °C to yield orange solid. The diffusion of pentane vapor into the concentrated solution of **5** in benzene yielded orange needles. Yield: 0.045 g (54%). X-ray quality single crystals of $\mathbf{5}^{meso}$ were obtained from the diffusion of pentane vapor into a concentrated benzene solution of $\mathbf{5}^{meso}$. Anal. Calcd for $C_{29}H_{28}N_2NiP_2\cdot(CH_2Cl_2)_{0.2}$: C, 64.69; H, 5.28; N, 5.17. Found: C, 64.46; H, 5.39; N, 5.22 (Note: ^{1}H NMR spectrum of $\mathbf{5}^{meso}$ contains ~0.05 equiv of residual CH_2Cl_2). ^{1}H NMR for $\mathbf{5}^{meso}$ (CD_2Cl_2, 400 MHz): δ 7.49 (m,P-Ph, 4H), 7.30 (m, Ar-H, 2H), 7.19 (m, P-Ph, 4H), 7.06 (m, Ar-H, 2H), 6.87 (m, Ar-H, 2H), 6.39 (m, Ar-H, 2H), 6.17 (m, Ar-H, 2H), 3.73 (m, NCH_2, 2H), 3.60 (m, NCH_2, 2H), 2.92 (m, PCH_2, 2H), 2.51 (m, $CH_2CH_2CH_2$, 1H), 1.80 (m, PCH_2, 2H), 1.35 (m, $CH_2CH_2CH_2$, 1H). ^{13}C{^{1}H} NMR for $\mathbf{5}^{meso}$ (CD_2Cl_2, 150.9 MHz): δ 165.1 (br), 133.4 (s), 132.5 (s), 132.3 (vt, $^2J_{PC}$ = 5 Hz), 130.8 (s), 129.8 (vt, $^1J_{PC}$ = 22 Hz), 128.9 (vt, $^2J_{PC}$ = 4 Hz), 120.0 (br), 112.0 (s), 109.7 (s), 54.8 (s, N*C*H$_2$), 24.8 (vt, $^1J_{PC}$ = 17 Hz, P*C*H$_2$CH$_2$*C*H$_2$P), 19.6 (s, PCH$_2$*C*H$_2$CH$_2$P). ^{31}P{^{1}H} NMR for $\mathbf{5}^{meso}$ (CD_2Cl_2, 162.0 MHz): δ 28.9 (s). ESI-MS *m/z*: calcd for $C_{29}H_{29}N_2NiP_2$ 525.1159; found 525.1132

{K(THF)$_x$}$_2$^{2Me}[PNNP]Ni (6). A mixture of **3** (0.20 g, 0.39 mmol) and KH (0.046 g, 1.15 mmol) in THF (20 mL) was heated at 50 °C for 72 h. The resulting dark red mixture was filtered through a pad of Celite and the filtrate was evaporated to dryness under vacuum. The residue was dissolved in THF (2 mL) and diffusion of pentane vapor into the resulting concentrated solution yielded **6** as a dark red solid. Crude yield: 0.18 g (~91%). X-ray quality single crystals were grown by decanting the mother liquor from the initial precipitation of **6**, followed by diffusion of pentane vapor into this THF solution. Although three K-coordinated THF molecules were present in the solid-state structure of **6** (x = 1.5), integration of the THF resonances in the ^{1}H NMR spectra of a dried samples of **6** are consistent with just one THF molecule (x = 0.5), Satisfactory elemental analysis data for **6** could not be obtained owing to its air and moisture sensitivity. ^{1}H NMR (THF-d_8, 400 MHz): δ 6.80 (m, Ar-H, 2H), 6.50 (m, Ar-H, 2H), 5.87 (m, Ar-H, 2H), 5.80 (m, Ar-H, 2H), 3.61 (m, THF, 4H), 3.30 (s, NCH_2, 4H), 1.77 (m, THF, 4H), 1.30 (br, PMe_2, 6H). ^{13}C{^{1}H} NMR (THF-d_8, 150.9 MHz): δ 162.1 (s), 145.0 (s), 130.6 (s), 124.7 (s), 109.1 (s), 105.2 (s), 68.2 (s, THF), 54.3 (s, N*C*H$_2$), 26.4 (s, THF), 10.1 (d, $^1J_{PC}$ = 28 Hz, PMe). ^{31}P{^{1}H} NMR (THF-d_8, 162.0 MHz): δ -3.5 (s).

^{4Me}[PNNP]Ni (7). To a frozen solution of **6** (0.047 g, 0.091 mmol) in THF (10 mL) inside a liquid N_2-cooled cold well was added MeI (0.033 g, 0.23 mmol). The reaction mixture was allowed to warm to room temperature and stirred for 2 h. The reaction mixture was filtered through a pad of Celite and the filtrate was evaporated to dryness under vacuum. The residue was extracted with toluene (6 mL) and filtered through a pad of Celite. The filtrate was reduced in volume to *ca.* 2 mL under vacuum. The diffusion of pentane vapor into the concentrated toluene solution yielded red-orange blocks and needles. Yield: 0.026 g (74 %). **Alternative one-pot synthesis**: A mixture of **3** (0.10 g, 0.20 mmol) and KH (0.023 g, 0.57 mmol) in THF (10 mL) was heated at 50 °C for 72 h. The reaction mixture was allowed to cool to room temperature, filtered through a pad of Celite, and frozen inside a liquid N_2-cooled cold well. MeI (0.071 g, 0.50 mmol) was added. The reaction mixture was allowed to warm to room temperature, stirred for 2 h, filtered through a pad of Celite, and evaporated to dryness under vacuum. The residue was extracted with toluene (6 mL) and filtered through a pad of Celite. The filtrate was reduced in volume to *ca.* 3 mL under vacuum and diffusion of pentane vapor into this concentrated toluene solution yielded red-orange blocks. Yield: 0.053 g (70%). ^{1}H NMR (C_6D_6, 400 MHz): δ 7.29 (m, Ar-H, 2H), 6.83 (m, Ar-H, 2H), 6.59 – 6.50 (m, two overlapping Ar-H signals, 4H), 3.68 (s, NCH_2, 4H), 0.82 (m, PMe_2, 12H). ^{13}C{^{1}H} NMR (C_6D_6, 150.9 MHz): δ 165.4 (vt, $^2J_{PC}$ = 13 Hz), 134.0 (s), 129.8 (s), 119.6 (vt, $^1J_{PC}$ = 28 Hz), 112.0 (s), 109.6 (vt, $^2J_{PC}$ = 8 Hz), 54.7 (s, N*C*H$_2$), 13.1 (vt, $^1J_{PC}$ = 14 Hz, PMe). ^{31}P{^{1}H} NMR (C_6D_6, 162.0 MHz): δ 13.5 (s). ESI-MS *m/z*: calcd for $C_{18}H_{25}N_2NiP_2$ 389.0846; found 389.0850.

H$_2$^{4Me}[PNNP] (8). To a stirring solution of **7** (0.085 g, 0.22 mmol) in CH_2Cl_2 (20 mL) were added degassed H_2O (10 mL) and KCN (2.52 g, 38.7 mmol). *Note: KCN could release a highly toxic chemical asphyxiant HCN. It should be handled only inside a fume hood and should not be mixed with an acid.* Stirring the mixture for 1 h turned the organic layer colorless and the aqueous layer orange-yellow. The organic layer was transferred to a new flask and dried over $MgSO_4$. The solution was filtered, and the solid was washed with CH_2Cl_2 (20 mL). The combined organic extracts were evaporated to dryness under vacuum and triturated with pentane 3 times. The residue was dissolved in a 1:1 mixture of Et_2O and pentane (4 mL) and stored at -35 °C to yield off-white needles. Yield: 0.053 g (73%). Anal. Calcd for $C_{18}H_{26}N_2P_2$: C, 65.05; H, 7.89; N, 8.43. Found: C, 64.96; H, 8.05; N, 8.32. ^{1}H NMR (C_6D_6, 400 MHz): δ 7.26 – 7.22 (m, Ar-H, 2H), 7.22 – 7.17 (m, Ar-H, 2H), 6.81 (m, Ar-H, 2H), 6.47 (m, Ar-H, 2H), 5.31 (br m, NH, 2H), 2.98 (m, NCH_2, 4H), 1.07 (d, $^2J_{PH}$ = 2.6 Hz, PMe_2, 12H). ^{13}C{^{1}H} NMR (C_6D_6, 150.9 MHz): δ 151.3 (d, $^1J_{PC}$ = 20 Hz), 130.4 (s), 129.8 (s), 124.2 (d, $^2J_{PC}$ = 9 Hz), 118.0 (s), 110.4 (s), 43.3 (s, N*C*H$_2$), 13.2 (d, $^1J_{PC}$ = 10 Hz, PMe). ^{31}P{^{1}H} NMR (C_6D_6, 162.0 MHz): δ -69.8 (s). ESI-MS *m/z*: calcd for $C_{18}H_{27}N_2P_2$ 333.1649; found 333.1646.

^{4Me}[PNNP]Pd (9). To a stirring suspension of $PdCl_2$ (0.016 g, 0.090 mmol) in THF (2 mL) was added a solution of **8** (0.030 g, 0.090 mmol) in THF (4 mL). The mixture was stirred overnight to yield a bright yellow precipitate. To the stirring suspension was added a solution of NaO^{t}Bu (0.018 g, 0.19 mmol) in THF (4

mL). A yellow solution formed immediately. The reaction mixture was stirred for 3 h, then filtered through a pad of Celite. The filtrate was evaporated to dryness under vacuum. The resulting yellow solid was dissolved in THF (4 mL), and diffusion of pentane vapor into the resulting solution formed yellow needles. Yield: 0.027 g (69%). Anal. Calcd for $C_{18}H_{24}N_2P_2Pd$: C, 49.50; H, 5.53; N, 6.41. Found: C, 49.67; H, 5.47; N, 6.38. ^{1}H NMR (CD_2Cl_2, 400 MHz): δ 7.06 (m, Ar-H, 2H), 7.00 (m, Ar-H, 2H), 6.37 – 6.28 (m, overlapping Ar-H signals, 4H), 3.59 (t, NCH_2, 4H, $^4J_{PC}$ = 1.4 Hz), 1.67 (m, PMe_2, 12H). ^{13}C{^{1}H} NMR (CD_2Cl_2, 150.9 MHz): δ 165.0 (m), 133.3 (s), 131.5 (s), 120.8 (m), 112.4 (vt, $^2J_{PC}$ = 4 Hz), 109.1 (vt, $^2J_{PC}$ = 10 Hz), 56.4 (s, N*C*H$_2$), 15.4 (m, PMe). ^{31}P{^{1}H} NMR (CD_2Cl_2, 162.0 MHz): δ 9.4 (s). ESI-MS *m/z*: calcd for $C_{18}H_{25}N_2P_2Pd$ 437.0528; found 437.0528.

Crystallographic Studies. Single crystals were mounted on a MiTeGen micromount using ParatoneN oil in air. The data were collected on a Bruker Nonius diffractometer with APEX II charge coupled detector (CCD) at 100(2) or 200(2) K using an Oxford Cryostreams low temperature device. The instrument was equipped with a graphite-monochromated Mo Kα radiation source. All manipulations including data collection, integration, scaling, and absorption corrections were carried out using the Bruker Apex2 software.[27] The structures were solved with Direct Methods (SHELXT)[28] and non-hydrogen atoms were confirmed with the least-square method (SHELXL).[29] Highly-disordered solvent molecules in **3** were eliminated using a solvent mask, which left two pockets with identical volume of 453.1 Å^3 and electron density of 83.0 e$^-$. The disordered carbon atoms (C17 and C18) in **4^{rac}** were refined over two positions with the sum of site occupancy factor of 1. The additional bond distance restraints were applied for adjacent C-C bond of 1.54 Å and C-O bond of 1.43 Å while the disorder was modeled. The twinned crystal of **6** was refined as a 2-component twin with the scales of 0.4936(10) and 0.5064(10). The positional disorder of carbon atoms (C47 and C48) in **6** were modeled by refining over two positions for each atom while setting the sum of site occupancy factor 1. The positions of all hydrogen atoms were idealized and they were allowed to ride on the attached carbon atoms. The final refinement included anisotropic temperature factor on all non-hydrogen atoms. Structure solution and refinement were performed with OLEX2,[30] and publication figures were generated with Mercury.[31] Crystallographic details are summarized in Table S1.

Computational Details. All calculations were performed using Gaussian16 for the Linux operating system.[32] DFT calculations were carried out using B3LYP hybrid functional[33,34] with a mixed basis set of def2-TZVP with effective core potentials for Ni,[35,36] 6-311+G(d) for N and P,[37,38] and D95V for C and H.[39] The crystal structures of **1**, **3^{rac}**, **4^{rac}**, and **5^{meso}** were used for the initial guess, and the geometry was optimized to a minimum. Subsequent frequency calculations were carried out to confirm the absence of imaginary frequencies and to obtain free energies and enthalpies. Transition state calculations were confirmed by intrinsic reaction coordinate calculations which led to each intermediate. Further details are summarized in Tables S2-S5, and XYZ coordinates are provided in Tables S6-S19.

ASSOCIATED CONTENT

Supporting Information

The Supporting Information is available free of charge on the ACS Publications website.

Crystallographic data, DFT calculation results, XYZ coordinates for optimized structures, NMR spectra of **3-9** and variable temperature reactions (PDF)

Accession Codes

CCDC 2105789-2105792 contain the supplementary crystallographic data for this paper. These data can be obtained free of charge via www.ccdc.cam.ac.uk/data_request/cif, or by e-mailing data_request@ccdc.cam.ac.uk, or by contacting The Cambridge Crystallographic Data Center, 12 Union Road, Cambridge CB2 1EZ, UK; fax: +44 1223 336033.

AUTHOR INFORMATION

Corresponding Author

* thomas.3877@osu.edu

Present Address

†K. Lee, Department of Chemical Education and Research Institute of Natural Sciences, Gyeongsang National University, Jinju 52828, Republic of Korea

ACKNOWLEDGMENT

This material is based upon work supported by the National Science Foundation under award number CHE-2101002. The Ohio State University Department of Chemistry and Biochemistry and The Ohio State Sustainability Institute are gratefully acknowledged for financial support. We would like to thank Dr. Curtis E. Moore and Dr. Alicia Friedman for their generous help in collecting the single crystal XRD and high resolution ESI-MS data, respectively. We thank Gillian P. Hatzis and Leah K. Oliemuller for insightful discussions.

REFERENCES

(1) *Phosphorus(III) Ligands in Homogeneous Catalysis: Design and Synthesis*; Kamer, P. C. J., Van Leeuwen, P. W. N. M., Eds.; John Wiley and Sons, 2012.

(2) *Organophosphorus Chemistry*; Allen, D. W., Loakes, D., Tebby, J. C., Eds.; Organophosphorus Chemistry; Royal Society of Chemistry: Cambridge, 2019; Vol. 48.

(3) *Phosphorus Ligands in Asymmetric Catalysis : Synthesis and Applications*; Börner, A., Ed.; Wiley-VCH, 2008.

(4) Tolman, C. A. Steric Effects of Phosphorus Ligands in Organometallic Chemistry and Homogeneous Catalysis. *Chem. Rev.* **1977**, *77* (3), 313–348.

(5) Perrin, L.; Clot, E.; Eisenstein, O.; Loch, J.; H. Crabtree, R. Computed Ligand Electronic Parameters from Quantum Chemistry and Their Relation to Tolman Parameters, Lever Parameters, and Hammett Constants. *Inorg. Chem.* **2001**, *40* (23), 5806–5811.

(6) J. Kendall, A.; R. Tyler, D. The Synthesis of Heteroleptic Phosphines. *Dalton Trans.* **2015**, *44* (28), 12473–12483.

(7) J. Kendall, A.; A. Salazar, C.; F. Martino, P.; R. Tyler, D. Direct Conversion of Phosphonates to Phosphine Oxides: An Improved Synthetic Route to Phosphines Including the First Synthesis of Methyl JohnPhos. *Organometallics* **2014**, *33* (21), 6171–6178.

(8) Day, G. S.; Pan, B.; Kellenberger, D. L.; Foxman, B. M.; Thomas, C. M. Guilty as Charged: Non-Innocent Behavior by a Pincer Ligand Featuring a Central Cationic Phosphenium Donor. *Chem. Commun.* **2011**, *47* (12), 3634–3636.

(9) Li, W.; Zhang, X. Chiral Phosphines and Diphosphines. In *Phosphorus(III) Ligands in Homogeneous Catalysis: Design and Synthesis*; Kamer, P. C. J., Leeuwen, P. W. N. M. van, Eds.; John Wiley & Sons, Ltd, 2012; pp 27–80.

(10) Li, Y.-Y.; Yu, S.-L.; Shen, W.-Y.; Gao, J.-X. Iron-, Cobalt-, and Nickel-Catalyzed Asymmetric Transfer Hydrogenation and Asymmetric Hydrogenation of Ketones. *Acc. Chem. Res.* **2015**, *48* (9), 2587–2598.

(11) Zuo, W.; Lough, A. J.; Li, Y. F.; Morris, R. H. Amine(Imine)Diphosphine Iron Catalysts for Asymmetric Transfer Hydrogenation of Ketones and Imines. *Science* **2013**, *342* (6162), 1080–1083.

(12) Mezzetti, A. Ruthenium Complexes with Chiral Tetradentate PNNP Ligands: Asymmetric Catalysis from the Viewpoint of Inorganic Chemistry. *Dalton Trans.* **2010**, *39* (34), 7851–7869.

(13) Bigler, R.; Huber, R.; Mezzetti, A. Highly Enantioselective Transfer Hydrogenation of Ketones with Chiral $(NH)_2P_2$ Macrocyclic Iron(II) Complexes. *Angew. Chem. Int. Ed.* **2015**, *54* (17), 5171–5174.

(14) Gautam, M.; Yatabe, T.; Tanaka, S.; Satou, N.; Takeshita, T.; Yamaguchi, K.; Nakajima, Y. Oxidative Addition of C–X Bonds and H–H Activation Using PNNP-Iron Complexes. *ChemistrySelect* **2020**, *5* (1), 15–17.

(15) Bestgen, S.; Schoo, C.; Neumeier, B. L.; Feuerstein, T. J.; Zovko, C.; Köppe, R.; Feldmann, C.; Roesky, P. W. Intensely Photoluminescent Diamidophosphines of the Alkaline-Earth Metals, Aluminum, and Zinc. *Angew. Chem. Int. Ed.* **2018**, *57* (43), 14265–14269.

(16) Tanaka, S.; Dubs, C.; Inagaki, A.; Akita, M. Polynuclear Rhodium Complexes with Dinucleating PNNP Ligand: Dynamic and Diverse M···M Interactions in [(μ-X)Rh2(PNNP)(CO)2]N+ and [(M4-X)Rh4(PNNP)2(CO)4]N+ [X = H, O, C≡C−R, R−C≡C−R, C≡C, CH=CH2, SMe2; n = 0, 1: PNNP = 3,5-Bis(Diphenylphosphinomethyl)Pyr. *Organometallics* **2004**, *24* (1), 163–184.

(17) Kounalis, E.; Lutz, M.; Broere, D. L. J. Cooperative H2 Activation on Dicopper(I) Facilitated by Reversible Dearomatization of an "Expanded PNNP Pincer" Ligand. *Chem. – A Eur. J.* **2019**, *25* (58), 13280–13284.

(18) Lee, K.; Moore, C. E.; Thomas, C. M. Synthesis of Ni(II) Complexes Supported by Tetradentate Mixed-Donor Bis(Amido)/Phosphine/Phosphido Ligands by Phosphine Substituent Elimination. *Organometallics* **2020**, *39* (11), 2053–2056.

(19) Hatzis, G. P.; Thomas, C. M. Metal-Ligand Cooperativity across Two Sites of a Square Planar Iron(II) Complex Ligated by a Tetradentate PNNP Ligand. *Chem. Commun.* **2020**, *56*, 8611–8614.

(20) Kuchen, W.; Buchwald, H. Umsetzungen Mit Diphenylphosphin-Natrium. *Angew. Chem.* **1957**, *69* (9), 307–308.

(21) Wittenberg, D.; Gilman, H. Notes - Lithium Cleavages of Triphenyl Derivatives of Some Group Vb Elements in Tetrahydrofuran. *J. Org. Chem.* **2003**, *23* (7), 1063–1065.

(22) Ye, J.; Zhang, J.-Q.; Saga, Y.; Onozawa, S.; Kobayashi, S.; Sato, K.; Fukaya, N.; Han, L.-B. Ready Approach to Organophosphines from ArCl via Selective Cleavage of C–P Bonds by Sodium. *Organometallics* **2020**, *39* (14), 2682–2694.

(23) Curtis, N. F. Macrocyclic Coordination Compounds Formed by Condensation of Metal-Amine Complexes with Aliphatic Carbonyl Compounds. *Coord. Chem. Rev.* **1968**, *3* (1), 3–47.

(24) Bennett, J.; Rae, A. D.; Salem, G.; Ward, N. C.; Waring, P.; Wells, K.; Willis, A. C. Synthesis of Bis[Palladium(II)] and Bis[Platinum(II)] Complexes Containing Chiral, Linear Quadridentate Ligands with a P2N2 Donor Set. *J. Chem. Soc. Dalt. Trans.* **2002**, No. 2, 234–243.

(25) Ansell, C. W. G.; Cooper, M. K.; Dancey, K. P.; Duckworth, P. A.; Henrick, K.; McPartlin, M.; Tasker, P. A. Template Synthesis of a New P_2N_2 Macrocyclic Ligand via Direct Alkylation of Co-Ordinated Amido Nitrogen Atoms; X-Ray Structure Analysis of the Free Ligand and Its Neutral Ni^{II} Complex. *J. Chem. Soc. Chem. Commun.* **1985**, No. 8, 439–441.

(26) Barclay, C. E.; Deeble, G.; Doyle, R. J.; Elix, S. A.; Salem, G.; Jones, T. L.; Wild, S. B.; Willis, A. C. Synthesis, Resolution and Reactions of (±)-(2-Aminophenyl)Methylphenylphosphine. Crystal and Molecular Structure of (R*,R*, S*, R*)-(±)-(1,3-Bis{[2-(Methylphenylphosphino)Phenyl]Amino}propane)Nickel(II) Perchlorate. *J. Chem. Soc. Dalt. Trans.* **1995**, *57* (1), 57–65.

(27) Bruker. Saint; SADABS; APEX3. Bruker AXS Inc.: Madison, Wisconsin, USA 2012.

(28) Sheldrick, G. M. SHELXT – Integrated Space-Group and Crystal-Structure Determination. *Acta Cryst.* **2015**, *A71*, 3–8.

(29) Sheldrick, G. M. Crystal Structure Refinement with SHELXL. *urn:issn:2053-2296* **2015**, *71* (1), 3–8.

(30) Dolomanov, O. V; Bourhis, L. J.; Gildea, R. J.; Howard, J. A. K.; Puschmann, H. OLEX2: A Complete Structure Solution, Refinement and Analysis Program. *J. Appl. Crystallogr.* **2009**, *42* (2), 339–341.

(31) Macrae, C. F.; Bruno, I. J.; Chisholm, J. A.; Edgington, P. R.; McCabe, P.; Pidcock, E.; Rodriguez-Monge, L.; Taylor, R.; van de Streek, J.;

Wood, P. A. Mercury CSD 2.0 - New Features for the Visualization and Investigation of Crystal Structures. *J. Appl. Crystallogr.* **2008**, *41* (2), 466–470.

(32) Frisch, M. J.; Trucks, G. W.; Schlegel, H. B.; Scuseria, G. E.; Robb, M. A.; Cheeseman, J. R.; Scalmani, G.; Barone, V.; Petersson, G. A.; Nakatsuji, H.; Li, X.; Caricato, M.; Marenich, A. V; Bloino, J.; Janesko, B. G.; Gomperts, R.; Mennucci, B.; Hratchian, H. P.; Ortiz, J. V; Izmaylov, A. F.; Sonnenberg, J. L.; Williams; Ding, F.; Lipparini, F.; Egidi, F.; Goings, J.; Peng, B.; Petrone, A.; Henderson, T.; Ranasinghe, D.; Zakrzewski, V. G.; Gao, J.; Rega, N.; Zheng, G.; Liang, W.; Hada, M.; Ehara, M.; Toyota, K.; Fukuda, R.; Hasegawa, J.; Ishida, M.; Nakajima, T.; Honda, Y.; Kitao, O.; Nakai, H.; Vreven, T.; Throssell, K.; Montgomery Jr., J. A.; Peralta, J. E.; Ogliaro, F.; Bearpark, M. J.; Heyd, J. J.; Brothers, E. N.; Kudin, K. N.; Staroverov, V. N.; Keith, T. A.; Kobayashi, R.; Normand, J.; Raghavachari, K.; Rendell, A. P.; Burant, J. C.; Iyengar, S. S.; Tomasi, J.; Cossi, M.; Millam, J. M.; Klene, M.; Adamo, C.; Cammi, R.; Ochterski, J. W.; Martin, R. L.; Morokuma, K.; Farkas, O.; Foresman, J. B.; Fox, D. J. Gaussian 16 Rev. C.01. Wallingford, CT 2016.

(33) Lee, C.; Yang, W.; Parr, R. G. Development of the Colle-Salvetti Correlation-Energy Formula into a Functional of the Electron Density. *Phys. Rev. B* **1988**, *37* (2), 785–789.

(34) Becke, A. D. Density-Functional Thermochemistr. III. The Role of Exact Exchange. *J. Chem. Phys.* **1993**, *98* (7), 5648–5652.

(35) Weigend, F.; Ahlrichs, R. Balanced Basis Sets of Split Valence, Triple Zeta Valence and Quadruple Zeta Valence Quality for H to Rn: Design and Assessment of Accuracy. *Phys. Chem. Chem. Phys.* **2005**, *7* (18), 3297–3305.

(36) Weigend, F. Accurate Coulomb-Fitting Basis Sets for H to Rn. *Phys. Chem. Chem. Phys.* **2006**, *8* (9), 1057–1065.

(37) Krishnan, R.; Binkley, J. S.; Seeger, R.; Pople, J. A. Self-consistent Molecular Orbital Methods. XX. A Basis Set for Correlated Wave Functions. *J. Chem. Phys.* **2008**, *72* (1), 650.

(38) McLean, A. D.; Chandler, G. S. Contracted Gaussian Basis Sets for Molecular Calculations. I. Second Row Atoms, Z=11–18. *J. Chem. Phys.* **2008**, *72* (10), 5639.

(39) Dunning, T. H.; Hay, P. J. No Title. In *Modern Theoretical Chemistry*; Schaefer, H. F., Ed.; Plenum: New York, 1976; Vol. 3, pp 1–28.

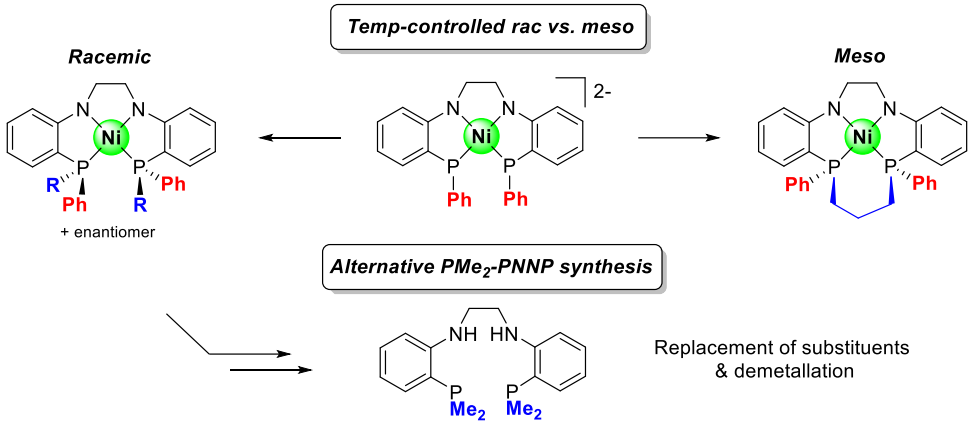
Temp-controlled rac vs. meso
Racemic
Meso
2-
+ enantiomer
Alternative PMe2-PNNP synthesis
Replacement of substituents
& demetallation